Nanoscale

COMMUNICATION

View Article Online
View Journal | View Issue

Cite this: *Nanoscale*, 2023, **15**, 19486

Received 10th August 2023,
Accepted 30th November 2023

DOI: 10.1039/d3nr04008a

rsc.li/nanoscale

Self-decorating cells *via* surface-initiated enzymatic controlled radical polymerization†

Andrea Belluati, *[a,b,c] Dominic Happel,[a] Malte Erbe,[a] Nicole Kirchner,[a] Anna Szelwicka,[a] Adrian Bloch,[a] Valeria Berner,[a] Andreas Christmann,[a] Brigitte Hertel,[d] Raheleh Pardehkhorram,[a] Amin Reyhani,[a] Harald Kolmar[a,b] and Nico Bruns *[a,b,c]

Through the innovative use of surface-displayed horseradish peroxidase, this work explores the enzymatic catalysis of both bioRAFT polymerization and bioATRP to prompt polymer synthesis on the surface of *Saccharomyces cerevisiae* cells, with bioATRP outperforming bioRAFT polymerization. The resulting surface modification of living yeast cells with synthetic polymers allows for a significant change in yeast phenotype, including growth profile, aggregation characteristics, and conjugation of non-native enzymes to the clickable polymers on the cell surface, opening new avenues in bioorthogonal cell-surface engineering.

Introduction

The application of nanotechnology is particularly exciting in the realm of biotechnology, where living cells can be interfaced with synthetic materials to achieve novel functionalities. Single-cell nanoencapsulation (SCNE) has great potential in augmenting the properties of individual cells by imparting orthogonal functionalities *via* decoration of the cell surface with non-natural molecules, effectively modifying the phenotype without altering their genetic makeup.[1] This has already been explored with microbial and animal cells,[2–9] *e.g.* by entrapping cells within enzyme-synthesized hydrogels.[10–12] Yeast cells, in particular, have proven to be a versatile subject for SCNE due to their broad range of biotechnological applications.[13–15] The well-known yeast surface display of enzymes on the membrane of *S. cerevisiae* provides a platform for *in situ* enzymatic reactions,[16,17] for instance with the enzyme horseradish peroxidase (HRP).[18] Surface-displayed HRP has been used to synthesize cross-linked phenol-modified alginate and chitosan hydrogels around yeast cells.[19] However, the resulting hydrogels were several micrometres thick, and their polymerization process was difficult to control. Linear polymer chains grafted to the cell surface form a shell with nanoscale thickness, thus providing a much thinner yet fully functional polymer sheath to the cells. Moreover, compared to crosslinked hydrogels, the defined structure of linear polymers offers easier tunability of thickness and density, as well as a broader range of surface functionalizations. Radical chain growth polymerization leads to linear polymers and can be carried out under cytocompatible conditions on living cells.[20–22] For example, polymer chains were grafted from living yeast cells through copper-catalysed atom transfer radical polymerization (ATRP),[13] or photoinduced electron transfer-reversible addition–fragmentation chain-transfer polymerization (PET RAFT).[23,24] However, the conditions used were relatively harsh and not easily scalable. ATRP and RAFT polymerizations can also be catalysed and initiated by enzymes such as HRP, hemoglobin, or laccases.[25–39] As enzymes can be produced by the cells themselves, bioATRP and bioRAFT polymerizations should be ideally suited to grow polymers on cell surfaces and, therefore, engineer the surface with enzymatically synthesized non-natural polymers.

Herein, we report the ability of HRP-displaying *S. cerevisiae* cells to polymerize monomers such as poly(ethylene glycol) methyl ether methacrylate (PEGMA), clickable PEGMA (bearing an azide group; PEGMA-N_3), and *N*-isopropyl acrylamide (NIPAM) on their cell surface (Fig. 1). To confine the polymerization to the surface of the cells, *i.e.* to form a nanoscale polymer layer around the cells, the polymerizations were carried out as grafting-from polymerization that forms polymer brushes. To this end, either a chain transfer agent (CTA) for RAFT polymerization or an alkyl halide ATRP initiator was chemically conjugated to the cell surface. With

[a]*Department of Chemistry, Technical University of Darmstadt, Peter-Grünberg-Straße 4, 64287 Darmstadt, Germany. E-mail: andrea.belluati@tu-darmstadt.de, nico.bruns@tu-darmstadt.de*
[b]*Centre for Synthetic Biology, Technical University of Darmstadt, Merckstraße 25, 64283 Darmstadt, Germany*
[c]*Department of Pure and Applied Chemistry, University of Strathclyde, Thomas Graham Building, 295 Cathedral Street, Glashow G1 1XL, UK*
[d]*Department of Biology, Technical University of Darmstadt, Schnittspahnstrasse 3, 64287 Darmstadt, Germany*

† Electronic supplementary information (ESI) available. See DOI: https://doi.org/10.1039/d3nr04008a

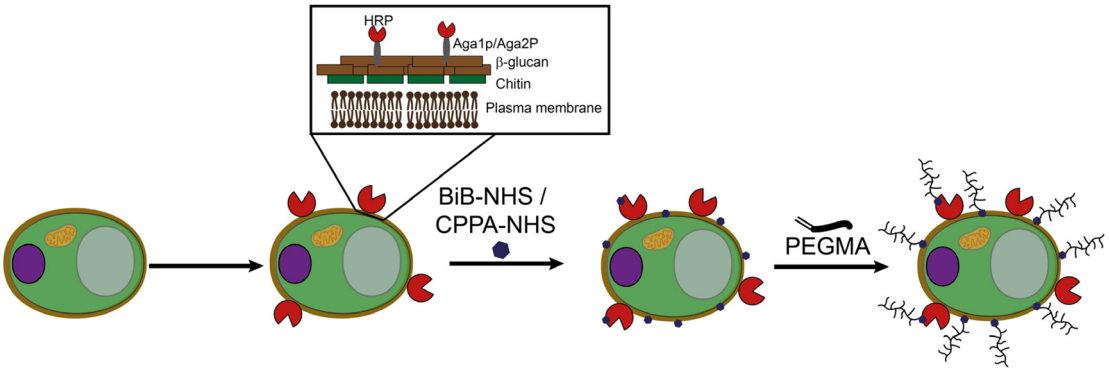

Fig. 1 Schematic of enzyme catalysed grafting-from polymerization on yeast cell surfaces: *S. cerevisiae* displays HRP (tethered to the proteins Aga1p–Aga2p) on the cell wall; the conjugation of either an ATRP initiator (BiB-NHS) or a RAFT chain transfer agent (CPPA-NHS) to surface proteins allows to graft polymer chains from the cell surface by HRP-catalysed bioATRP or bioRAFT of vinyl monomers, such as the macromonomer PEGMA.

PEGMA as a macromonomer, the resulting polymers are highly hydrophilic and biocompatible,[40] making them desirable for biological applications. In addition, the clickable monomer allows the polymer brushes to be functionalized with fluorescent dyes and non-native enzymes. Thus, the cells can self-encapsulate in a synthetic polymer, allowing for bioorthogonal engineering of the cell surface, *e.g.*, for the cells to acquire new metabolic capabilities or to be used as building blocks for engineered living materials.

Results and discussion

Polymerization conditions for bioATRP and bioRAFT on yeast cells

We expressed HRP on the surface of *S. cerevisiae* and grew the yeast on synthetic galactose-containing medium (SG). Flow cytometry data showed that 40% of the yeast cells expressed the enzyme, resulting in two populations (with and without HRP). This expression level aligns with typical findings in yeast surface display (ESI Fig. 1a†).[41] The 3,3′,5,5′-tetramethylbenzidine (TMB) peroxidase activity assay[42] showed that HRP-expressing cultures had much higher enzymatic activity than the control, suggesting that the surface-displayed enzyme could be investigated as a catalyst for biocatalytic controlled radical polymerization (ESI Fig. 1b†). We tested enzymatic RAFT (bioRAFT) and ATRP (bioATRP) for enzyme-mediated polymerizations. To this end, *N*-hydroxysuccinimide (NHS) chemistry was used to tether either the RAFT chain transfer agent 4-cyano-4-(phenylcarbonothioylthio)pentanoic acid (CPPA) or the ATRP initiator bromoisobutyrate (BiB) to lysines exposed on the surface of the yeast cells. The fluorescamine assay showed that nearly 90% of both the added chain transfer agent or the initiator were conjugated to the cell surface (ESI Fig. 2†). Using carboxyfluorescein-NHS (CF-NHS) as a fluorescent model molecule with similar reactivity, we observed no visible uptake into the cells, suggesting that both CPPA and BiB would be presented on the outer cell surface, together with the surface-displayed HRP (ESI Fig. 3†).

We then proceeded to compare the monomer conversion, as well as the number-average molecular weight (M_n) and dispersity ($Đ$) of PPEGMA that was synthesized on the cells at 37 °C but in otherwise different conditions. To this end, PPEGMA was detached from the proteins after the polymerization and characterized by NMR spectroscopy (monomer conversion) and gel permeation chromatography (M_n and $Đ$) (Table 1 and ESI Fig. 4†). In the absence of surface-displayed HRP and initiator or CTA, the monomer conversion was low (**P1**). Polymerizations were carried out with the initiators free in solution (1-step process: conjugation simultaneously with polymerization) or tethered to the surface (2-step protocol: polymerization after conjugation) (**P2** and **P3** *vs.* **P4** and **P5**, ESI Fig. 5†). The 2-step protocol achieved better conversion and resulted in polymers with lower dispersity. Cells performing ATRP also consistently showed a better viability (generally >70%) than cells subjected to RAFT polymerization (<50% viability) (ESI Fig. 6†), as well as better monomer conversion and comparable dispersity. A control experiment with the initiator but without expressed HRP showed low but non-negligible monomer conversion (23%), suggesting residual activity on the surface of yeast (**P6**). Interestingly, when free HRP was added in solution to cells that did not display the enzyme on their surface (at the same concentration as it would have been expressed by the yeast, ~5.3 μg mL^{-1}), a similarly low conversion was observed (**P7**, ESI Fig. 7†). Thus, the low amount of HRP in the reaction mixture did not have effect on the conversion, which highlights that the mere presence of HRP in solution is not sufficient for efficient conversion. The display of HRP on the yeast surface significantly enhances efficiency of the reaction, probably by locally creating high enzyme concentrations on the yeast. This was further confirmed by confining HRP on one kind of cell, and the polymers on another: HRP-displaying yeast were combined with yeast cells lacking HRP but possessing the ATRP initiator (ESI Fig. 8†). The monomer conversion remained low, showing that no inter-cell polymerization occurred (**P8**). Thus, the efficient polymerization on the cell surface requires both the enzyme and the initiator on the same cell.

Table 1 Summary of the main polymerization conditions and the resulting monomer conversion, molecular weight and dispersity of polymers that were enzymatically synthesized on the surface of yeast. The monomer to initiator/CTA was 20 : 1, except in **P11** (*vide infra*)

Name	1 step/2 step conjugation	Medium	Type of polymerization	HRP expression	Monomer	Monomer conversion (%)	M_n (g mol^{-1}) (theoretical)	M_n (g mol^{-1}) (GPC)	$Đ$ (GPC)
P1	—[a]	PBS	—	−	PEGMA	7	3329	53 317	2.66
P2	1	PBS	ATRP	+	PEGMA	75	34 383	71 510	2.95
P3	1	PBS	RAFT	+	PEGMA	45	20 717	40 015	1.95
P4	2	PBS	ATRP	+	PEGMA	74	33 850	36 157	1.33
P5	2	PBS	RAFT	+	PEGMA	57	25 617	26 891	1.61
P6	2	PBS	ATRP	−	PEGMA	23	11 797	52 583	1.76
P7	2	PBS	ATRP	−[b]	PEGMA	26	12 048	55 726	1.67
P8	2[c]	PBS	ATRP	±	PEGMA	22	10 207	45 123	2.47
P9	2	YPD	ATRP	+	PEGMA	94	42 957	33 671	1.62
P10	2	YPD	RAFT	+	PEGMA	81	37 172	36 503	1.69
P11	2	YPD	ATRP	+	PEGMA : PEGMA-N_3 (3 : 1)	93	34 734	35 637	1.48
P12	2	YPD	ATRP	+	PEGMA : PEGMA-N_3 (9 : 1)[d]	97	9952	48 641	1.55
P13	2	YPD	ATRP	+	PEGMA : PEGMA-N_3 (3 : 1)[d]	50	20 163	56 102	2.04
P14	2	YPD	ATRP	+	PEGMA-N_3	93	21 409	48 840	1.16
P15	2	YPD	ATRP	+	NIPAM	50	13 040	37 245	1.3
P16	2	YPD	ATRP	+	PEGMA-Cy5	96	42 095	57 521	1.2

PBS: phosphate-buffered saline. YPD: yeast–peptone–dextrose. [a] No initiator/CTA added, used as negative control. [b] Free HRP added to uninduced yeast. [c] NHS-BiB conjugated to cells not expressing HRP, mixed with cells expressing HRP but without initiator. [d] Chain extension in **P13** of the polymers synthesized in **P12**.

We then switched the polymerization from PBS to yeast–peptone–dextrose culture media (YPD), where we could polymerize PEGMA almost quantitatively (**P9**) *via* the ATRP mechanism, probably due to a higher reductive environment thanks to the increased cell metabolism. Also RAFT polymerization achieved improved monomer conversion (**P10**).

The most striking feature in YPD was the greatly increased viability of the cells for ATRP (>80%), whereas RAFT could only achieve 51% (ESI Fig. 6†). Thus, we focused on ATRP in YPD for the ensuing polymerizations.

For instance, it was also possible to co-polymerize PEGMA bearing an azide group (PEGMA-N_3) (**P11**), setting the groundwork for surface conjugation. We observed that the zeta potential (ζ-potential) of the modified yeast cells remained relatively consistent when comparing naked (polymer-less) cells to those with attached polymers. This suggests that the surface-attached polymers, likely due to the water-soluble nature of PEG and its inherent steric effects, may not densely cover the cell surface, thereby having minimal impact on the zeta potential (ESI Fig. 9†).

Furthermore, we tested whether the polymer chains could be extended in a subsequent polymerization: in **P12**, a first PPEGMA : PPEGMA-N_3 (9 : 1 molar) polymer was produced on the cell surface. The same cells were then subjected to another iteration of a similar copolymerization (**P13**) (Table 1 and ESI Fig. 10†). The monomer conversion was lower than in the first step, the number average molecular weight increased slightly, and $Đ$ increased from 1.55 to above 2. Moreover, the experimental M_n were much higher than the theoretical values in both steps. These results suggest that, while polymers could be chain extended, the initiation of this step was inefficient, and only a few chains tended to grow to a maximum length. Thus, while bioATRP on yeast cell surface can produce relatively narrowly dispersed polymers, they tend to be irreversibly deactivated.

We observed that the zeta potential (ζ-potential) of the modified yeast cells remained relatively consistent when comparing naked (polymer-less) cells to those with attached polymers (ESI Fig. 9†). This suggests that the surface-attached polymers, likely due to the water-soluble nature of PEG and its inherent steric effects, may not densely cover the cell surface, thereby having minimal impact on the zeta potential.

To assess the ability of yeast to undergo polymerization across multiple generations, *i.e.*, to consistently self-encapsulate even after shedding part of their polymer coating during budding, the PPEGMA of **P14** cells were labelled with Cy5 (*vide infra*), after which the yeast cells were allowed to grow for further 36 h on SG. As expected, flow cytometry showed that the original polymer coating had been "diluted" across generations, and most yeast cells were lacking fluorescently labelled polymers. A new polymerization of PEGMA-N_3 again resulted in a high conversion (88%) and allowed the labelling of the polymer-coated cells with Cy5. The resulting population of fluorescently labelled cells showed very similar flow cytometry results to the original generation of polymer-functionalized cells, confirming the ability to repeat the enzymatic polymerization process *ad libitum* (ESI Fig. 12†). This mimics the natural ability of yeast cells to reform the cell wall after replication, and the result is crucial for potential applications of self-encapsulating yeast, for example in whole-cell biocatalysis.[8]

Finally, we explored the use of *N*-isopropylacrylamide (NIPAM) for polymerization, creating **P15**, a polymer variant

with a lower monomer conversion but still a good control over polymerization, which offers a different set of properties for potential applications beyond those achieved with PEGMA-based systems.

Engineering of the cell surface with PPEGMA

Having confirmed the successful formation of polymer brushes on the yeast cells, we moved on to characterize the effect it would have on the microbes. **P9** cells exhibited a slightly slower and limited growth (Fig. 2a). In addition, the PPEGMA layer increased the number of surviving yeast cells when treated with zymolyase (Fig. 2b), most likely because it hindered, to an extent, the digestion of the cell wall by this enzyme.

TEM images of **P9** showed that yeast had darker sections on its cell wall, compared to naked yeast, possibly due to the adsorption of the staining agent on PPEGMA (ESI Fig. 11†). To further confirm the presence of PPEGMA on the surface of yeast, we incubated **P9** and naked yeast with fluorescently-labelled concanavalin A (TAMRA-ConcA) (ESI Fig. 13a†). ConcA is a protein that binds specifically to carbohydrate residues which are abundant on the outer surface of yeast cell walls. We hypothesized that if PPEGMA was present on the yeast surface, there would be a reduced accessibility of these mannose and glucose residues due to the steric hindrance provided by the polymer chains, and consequently, a decreased fluorescence when compared to naked yeast. Using fluorescence microscopy, we observed a noticeable reduction in TAMRA-ConcA binding on **P9** cells compared to naked yeast (ESI Fig. 13b and c†), which was quantitatively confirmed by fluorimetry (ESI Fig. 13d†). This not only indicates that PPEGMA was present on the yeast surface but also suggests a dense grafting of the polymer chains that limits the accessibility of the underlying cell wall components to external molecules such as ConcA.

As previously reported, tannic acid (TA) can non-covalently crosslink PEG chains on cell surfaces.[23] Addition of TA to the polymer-decorated yeast cells resulted in large yeast clusters due to this crosslinking (ESI Fig. 14†). Upon centrifugation and subsequent washing with PBS, TA was removed, resulting in the yeast cells becoming disperse again (ESI Fig. 14†). Thus, the polymer coating could influence the aggregation behaviour of cells.

In our quest to explore the potential applications of the polymer-decorated yeast cells, we became interested in the ability to generate metallic nanoparticles (NPs) on the cell surface, since yeast cells are also known as efficient, "green" synthesizers of NPs,[43] and this has potential relevance in areas such as catalysis, biosensing, and environmental remediation. We hypothesized that the polymer brushes might serve as an effective matrix for NP synthesis and stabilization on the cells (ESI Fig. 15a†).[44] In the case of silver nanoparticles (AgNP), the particles harvested from the supernatant were 13× more abundant using **P9** than the naked yeast (ESI Fig. 15b and c†) and their ζ-potential was more neutral (ESI Fig. 15d†), a clear sign of the impact of PPEGMA. Nevertheless, AgNP are biocides,[45] and their production did affect cell viability, which dropped to less than 50% for the cells with PPEGMA (ESI Fig. 15e†). The yield of palladium nanoparticles (PdNP),[46] on the other hand, was 2× higher than in the controls (ESI Fig. 16a†), and viability was not affected (ESI Fig. 16b†).

Taken together, our findings not only confirm the successful formation of a PPEGMA polymer brush on yeast cells, but also reveal a multifaceted interplay between the polymer and the cellular behaviour. The modification of the cells with polymers impacts cell growth, imparts resistance to enzymatic degradation, alters response to crosslinking agents, and modulates the cell's capacity for nanoparticle synthesis.

On-surface polymer functionalization

The presence of azide groups on P(PEGMA-*co*-PEGMA-N_3) polymers provides a powerful tool for the attachment of various functional molecules *via* click chemistry to the cells, further extending the application potential of these modified yeast cells. To demonstrate this, a clickable fluorescent dye (Cy5-dibenzocyclooctyne, Cy5-DBCO) was incubated with **P11** cells and **P14** cells. The successful conjugation was confirmed *via* confocal microscopy and flow cytometry (Fig. 3a, b and ESI Fig. 17†). Cy5 fluorescence was detected on the surface of yeast. However, flow cytometry showed a rather poor labelling

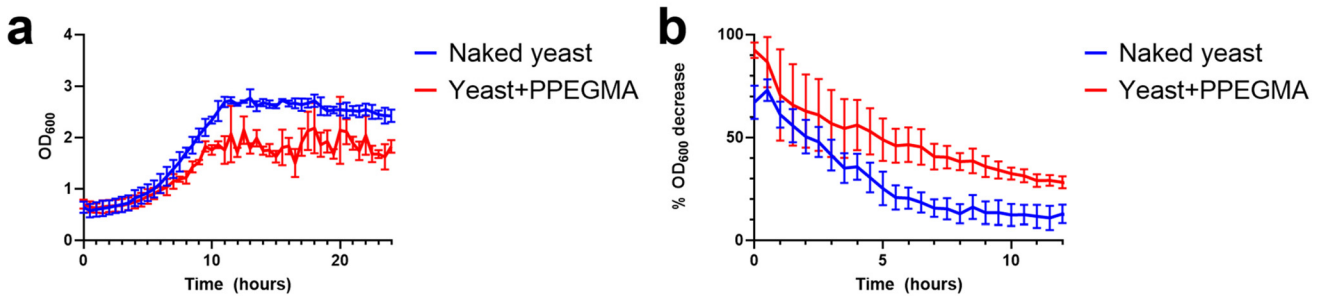

Fig. 2 Influence of the enzymatically synthesized PPEGMA on the growth and resistance against enzymatic lysis of yeast cells. (a) OD_{600} curve for naked and PPEGMA-coated *S. cerevisiae*. (b) % OD_{600} curve for naked and PPEGMA-coated *S. cerevisiae* incubated with zymolyase. Mean values, and error bars displayed as SD, n = 3.

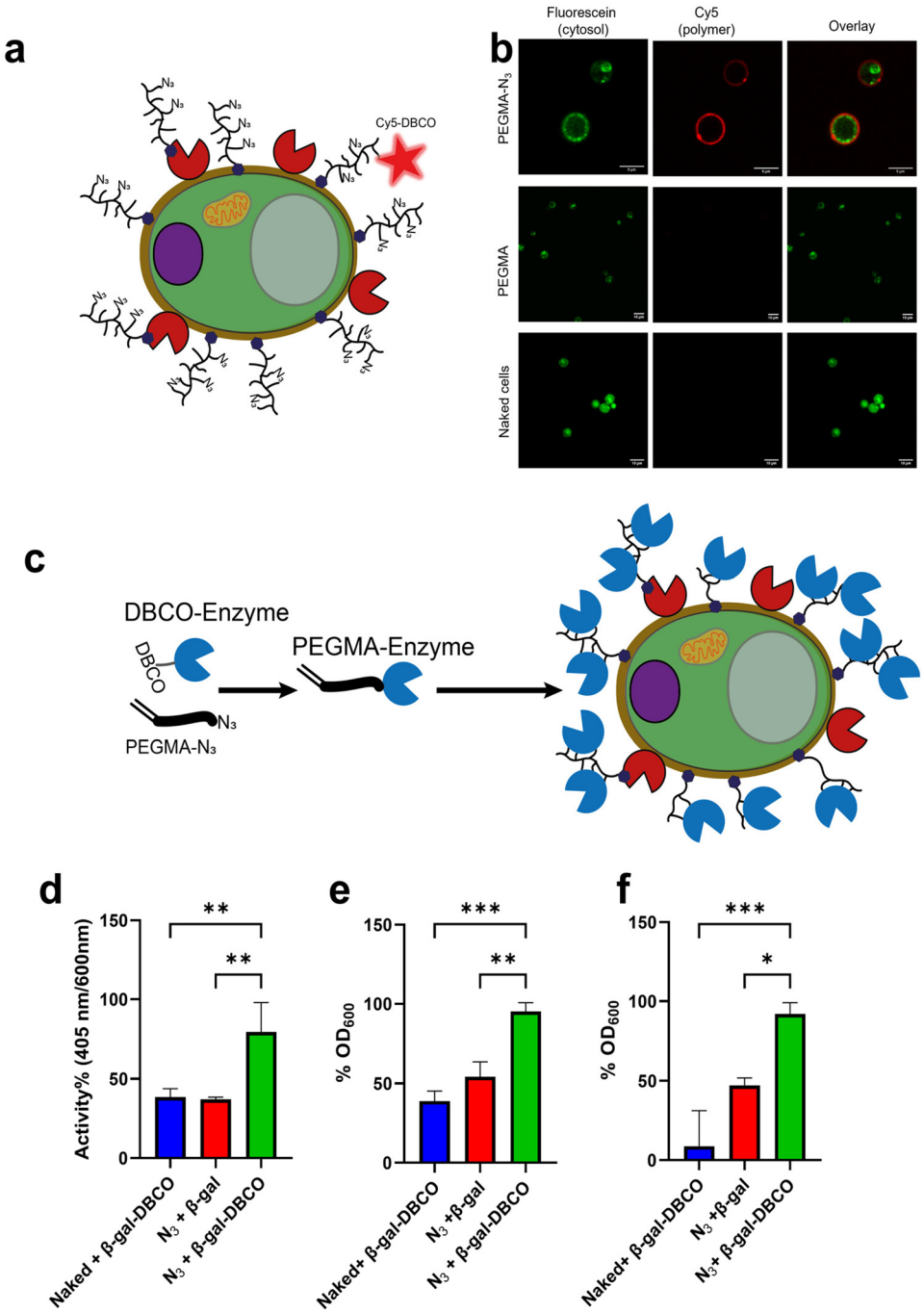

Fig. 3 Biorthogonal functionalization of yeast cells through click-chemistry conjugation to the polymer PPEGMA-N_3 on the cell surface or by polymerizing functionalized PEGMA-N_3 monomers. (a) Scheme of the conjugation of fluorescent Cy5 to PPEGMA-N_3. (b) CLSM micrographs of Cy5-conjugated cells. Scale bars: 5 μm (PEGMA-N_3), 10 μm (other micrographs). (c) Scheme of the conjugation of enzymes (*e.g.* β-gal) to PEGMA and subsequent polymerization. Note that some enzymes might be conjugated to more than one PPEGMA chain, effectively crosslinking the polymers. (d) Results of the colorimetric activity assay for β-gal: activity (normalized % absorbance 405 nm/OD_{600}) for naked cells incubated with β-gal (blue), yeast with PEGMA-N_3 polymerized in presence of β-gal without DBCO (thus unclickable, red) and β-gal conjugated to PEGMA-N_3, *i.e.* β-gal-functionalized yeast. (e) Enhanced cell growth by digestion of lactose through β-gal: % OD_{600} for β-gal-conjugated yeast incubated in lactose medium (YPL). (f) Enhanced cell survival in the presence octyl-glucopyranoside by β-gal: % OD_{600} for β-gal-conjugated yeast incubated with 25 mM octyl-glucopyranoside. Mean values, error bars displayed as SD, $n = 3$. **: $p < 0.01$, ***: $p < 0.001$.

efficiency suggesting a low incorporation of PEGMA-N_3 into these copolymers (ESI Fig. 18†). We then focused our attention on the PPEGMA-N_3 homopolymer (**P14**) in order to increase the number of fluorescent dyes on the cells. Cy5 was once again successfully conjugated to the polymers (ESI Fig. 19 and 20†).

To augment the cells with non-native functionality, proteins were conjugated to the clickable polymers using enzymes that were modified with a cycloalkyne linker.[8,47,48] We selected the enzyme β-galactosidase (β-gal), as it is not expressed by *S. cerevisiae*. The *post hoc* conjugation of β-gal-DBCO to **P14** proved to be ineffective, possibly hindered by the protein-repellent PEG brushes (ESI Fig. 21a†). Thus, we tested the possibility of using PEGMA-N_3 monomers to which functional entities were conjugated before polymerization. In a first test, Cy5 was clicked to azide-PEGMA and then the monomer was polymerized on the cell surface (**P16**). The fluorescence could once again be detected on the yeast surface, demonstrating that modified macromonomers could be polymerized on the cells (ESI Fig. 22†). We then conjugated β-gal to the macromonomer before polymerization, with a conjugation efficiency of 33% (Fig. 3c and ESI Fig. 21a, b†). Not only were β-gal-functionalized yeast cells able to yield the coloured *o*-nitrophenol from a chromogenic substrate of β-gal (Fig. 3d), but the enzyme could also increase the proliferation of yeast on lactose as the main carbon source (Fig. 3e) which the cells would otherwise not be able to metabolize as they do not express this enzyme. Moreover, β-gal improved the survival of the cells against the detergent octyl-glucopyranoside (Fig. 3f), as the enzyme degrades this compound.[49]

To prove the versatility of the approach to functionalize cell surfaces with polymer–enzyme conjugates, alkaline phosphatase (ALP), an enzyme that also is not excreted by the yeast, was linked to the clickable monomer, which was then polymerized on the cells (ESI Fig. 21†). ALP too made the decorated cells produce *o*-nitrophenol; furthermore, the enzyme was able to induce the precipitation of calcium phosphate by cleaving the substrate calcium glycerophosphate,[39] resulting in mineral clusters depositing around the cells, thus creating a novel mechanism for biomineralization mediated by *S. cerevisiae* (ESI Fig. 23b†).[50]

Concluding, the experiments with the two model enzymes show that self-synthesized polymer–enzyme conjugates can be used to install orthogonal catalytic activity onto yeast cells which strongly modifies the behaviour of the cells.

Conclusions

In conclusion, we show how the yeast surface display of HRP can be exploited to create *S. cerevisiae* cells that can synthesize polymers on their surface through enzymatic controlled radical polymerizations. The cells encapsulate themselves in a synthetic polymer and are able to repeat such a process across generations to renew the polymer coating. The mild reaction conditions are cytocompatible and allow for high cell viability. The polymers alter the behaviour of the cells and allow the bioorthogonal functionalization of the cell surface, *e.g.* with non-native enzymes, thus broadly changing the possible phenotypes by the introduction of just a single enzyme. Such hybrid cells could find applications as whole-cell biocatalysts that have acquired new metabolic capabilities, or as building blocks for engineered living materials such as self-replicating yeast–polymer composites. Methodological adjustments will allow the concept to be applied to other cell types such as animal cells that lack a chitin wall. Thus, our work blurs the boundary between natural and synthetic matter, with implications for both materials science and biotechnology.

Data availability

The datasets generated and analysed during the current study are available in the Zenodo repository **https://doi.org/10.5281/zenodo.10223638**.

Author contributions

A. B.: conceptualization, methodology, investigation, data analysis and interpretation, writing – original draft, visualization, funding acquisition, supervision. D. H.: methodology, investigation, formal analysis. M. E.: investigation, validation. N. K.: investigation, validation. A. S.: investigation, methodology, writing – review & editing. A. B.: investigation, validation. V. B.: investigation, validation. A. C.: methodology, investigation, supervision, methodology. B. H.: investigation, data analysis. R. P.: investigation, validation. H. K.: funding acquisition, supervision, resources. N. B.: conceptualization, project administration, writing – review & editing, resources, supervision, funding acquisition. All authors reviewed and edited the manuscript.

Conflicts of interest

There are no conflicts to declare.

Acknowledgements

This project received funding from the European Union's Horizon 2020 research and innovation program under the Marie Skłodowska-Curie grant agreement no. 101032493 and UK Engineering and Physical Sciences Research Council (grant numbers EP/V047035/1 and EP/V047035/2). The authors acknowledge the funding provided by ULB Darmstadt for publication.

Notes and references

1 W. Youn, J. Y. Kim, J. Park, N. Kim, H. Choi, H. Cho and I. S. Choi, *Adv. Mater.*, 2020, **32**, 1907001.
2 C. Delneuville, E. P. Danloy, L. Wang and B.-L. Su, *J. Sol-Gel Sci. Technol.*, 2019, **89**, 244–254.
3 R. F. Fakhrullin and R. T. Minullina, *Langmuir*, 2009, **25**, 6617–6621.

4 W. Geng, N. Jiang, G.-Y. Qing, X. Liu, L. Wang, H. J. Busscher, G. Tian, T. Sun, L.-Y. Wang, Y. Montelongo, C. Janiak, G. Zhang, X.-Y. Yang and B.-L. Su, *ACS Nano*, 2019, **13**, 14459–14467.
5 E. H. Ko, Y. Yoon, J. H. Park, S. H. Yang, D. Hong, K.-B. Lee, H. K. Shon, T. G. Lee and I. S. Choi, *Angew. Chem., Int. Ed.*, 2013, **52**, 12279–12282.
6 S. A. Konnova, A. A. Danilushkina, G. I. Fakhrullina, F. S. Akhatova, A. R. Badrutdinov and R. F. Fakhrullin, *RSC Adv.*, 2015, **5**, 13530–13537.
7 V. Kozlovskaya, S. Harbaugh, I. Drachuk, O. Shchepelina, N. Kelley-Loughnane, M. Stone and V. V. Tsukruk, *Soft Matter*, 2011, **7**, 2364–2372.
8 A. Belluati, I. Harley, I. Lieberwirth and N. Bruns, *Small*, 2023, 2303384, DOI: **10.1002/smll.202303384**.
9 L. Feng, L. Gao, D. F. Sauer, Y. Ji, H. Cui and U. Schwaneberg, *Chem. Commun.*, 2021, **57**, 4460–4463.
10 R. Vanella, A. Bazin, D. T. Ta and M. A. Nash, *Chem. Mater.*, 2019, **31**, 1899–1907.
11 Y. Liu, S. Sakai, S. Kawa and M. Taya, *Anal. Chem.*, 2014, **86**, 11592–11598.
12 S. Sakai, Y. Liu, M. Sengoku and M. Taya, *Biomaterials*, 2015, **53**, 494–501.
13 J. Y. Kim, B. S. Lee, J. Choi, B. J. Kim, J. Y. Choi, S. M. Kang, S. H. Yang and I. S. Choi, *Angew. Chem., Int. Ed.*, 2016, **55**, 15306–15309.
14 N. Kim, H. Lee, S. Y. Han, B. J. Kim and I. S. Choi, *Appl. Surf. Sci. Adv.*, 2021, **5**, 100098.
15 H. C. Moon, S. Han, J. Borges, T. Pesqueira, H. Choi, S. Y. Han, H. Cho, J. H. Park, J. F. Mano and I. S. Choi, *Soft Matter*, 2020, **16**, 6063–6071.
16 G. M. Cherf and J. R. Cochran, *Methods Mol. Biol.*, 2015, **1319**, 155–175.
17 S. Fan, B. Liang, X. Xiao, L. Bai, X. Tang, E. Lojou, S. Cosnier and A. Liu, *J. Am. Chem. Soc.*, 2020, **142**, 3222–3230.
18 D. Lipovsek, E. Antipov, K. A. Armstrong, M. J. Olsen, A. M. Klibanov, B. Tidor and K. D. Wittrup, *Chem. Biol.*, 2007, **14**, 1176–1185.
19 R. Vanella, A. Bazin, D. T. Ta and M. A. Nash, *Chem. Mater.*, 2019, **31**, 1899–1907.
20 P. Laskar, O. P. Varghese and V. P. Shastri, *Adv. NanoBiomed Res.*, 2023, 2200174.
21 Z. Zhou, K. Maxeiner, D. Y. W. Ng and T. Weil, *Acc. Chem. Res.*, 2022, **55**, 2998–3009.
22 X. Zhang, J. Wang, Y. Zhang, Z. Yang, J. Gao and Z. Gu, *Chem. Soc. Rev.*, 2023, **52**, 8126–8164.
23 J. Niu, D. J. Lunn, A. Pusuluri, J. I. Yoo, M. A. O'Malley, S. Mitragotri, H. T. Soh and C. J. Hawker, *Nat. Chem.*, 2017, **9**, 537–545.
24 M. Zhu, S. Wang, Z. Li, J. Li, Z. Xu, X. Liu and X. Huang, *Nat. Commun.*, 2023, **14**, 3598.
25 S. J. Sigg, F. Seidi, K. Renggli, T. B. Silva, G. Kali and N. Bruns, *Macromol. Rapid Commun.*, 2011, **32**, 1710–1715.
26 T. B. Silva, M. Spulber, M. K. Kocik, F. Seidi, H. Charan, M. Rother, S. J. Sigg, K. Renggli, G. Kali and N. Bruns, *Biomacromolecules*, 2013, **14**, 2703–2712.
27 C. Fodor, B. Gajewska, O. Rifaie-Graham, E. A. Apebende, J. Pollard and N. Bruns, *Polym. Chem.*, 2016, **7**, 6617–6625.
28 M. Divandari, J. Pollard, E. Dehghani, N. Bruns and E. M. Benetti, *Biomacromolecules*, 2017, **18**, 4261–4270.
29 K. J. Rodriguez, B. Gajewska, J. Pollard, M. M. Pellizzoni, C. Fodor and N. Bruns, *ACS Macro Lett.*, 2018, **7**, 1111–1119.
30 Y.-H. Ng, F. di Lena and C. L. L. Chai, *Polym. Chem.*, 2011, **2**, 589–594.
31 Y.-H. Ng, F. di Lena and C. L. L. Chai, *Chem. Commun.*, 2011, **47**, 6464–6466.
32 G. Gao, M. A. Karaaslan, J. F. Kadla and F. Ko, *Green Chem.*, 2014, **16**, 3890–3898.
33 B. Zhang, X. Wang, A. Zhu, K. Ma, Y. Lv, X. Wang and Z. An, *Macromolecules*, 2015, **48**, 7792–7802.
34 Z. Liu, Y. Lv and Z. An, *Angew. Chem., Int. Ed.*, 2017, **56**, 13852–13856.
35 R. Li, W. Kong and Z. An, *Angew. Chem., Int. Ed.*, 2022, e202202033, DOI: **10.1002/anie.202202033**.
36 R. Li, W. Kong and Z. An, *Macromolecules*, 2023, **56**, 751–761.
37 A. P. Danielson, D. B. Van Kuren, M. E. Lucius, K. Makaroff, C. Williams, R. C. Page, J. A. Berberich and D. Konkolewicz, *Macromol. Rapid Commun.*, 2016, **37**, 362–367.
38 A. P. Danielson, D. B. Van-Kuren, J. P. Bornstein, C. T. Kozuszek, J. A. Berberich, R. C. Page and D. Konkolewicz, *Polymers*, 2018, **10**(7), 741.
39 A. Belluati, S. Jimaja, R. J. Chadwick, C. Glynn, M. Chami, D. Happel, C. Guo, H. Kolmar and N. Bruns, *Nat. Chem.*, 2023, DOI: **10.1038/s41557-023-01391-y**.
40 X. Y. Liu, J. M. Nothias, A. Scavone, M. Garfinkel and J. M. Millis, *ASAIO J.*, 2010, **56**, 241–245.
41 K. V. Teymennet-Ramírez, F. Martínez-Morales and M. R. Trejo-Hernández, *Front. Bioeng. Biotechnol.*, 2022, **9**, 794742.
42 V. R. Holland, B. C. Saunders, F. L. Rose and A. L. Walpole, *Tetrahedron*, 1974, **30**, 3299–3302.
43 A. Boroumand Moghaddam, F. Namvar, M. Moniri, P. Md Tahir, S. Azizi and R. Mohamad, *Molecules*, 2015, **20**, 16540–16565.
44 C. Luo, Y. Zhang, X. Zeng, Y. Zeng and Y. Wang, *J. Colloid Interface Sci.*, 2005, **288**, 444–448.
45 Y. N. Slavin and H. Bach, *Nanomaterials*, 2022, **12**, 4470.
46 N. Saitoh, R. Fujimori, T. Yoshimura, H. Tanaka, A. Kondoh, T. Nomura and Y. Konishi, *Hydrometallurgy*, 2020, **196**, 105413.
47 V. Maffeis, A. Belluati, I. Craciun, D. Wu, S. Novak, C.-A. Schoenenberger and C. G. Palivan, *Chem. Sci.*, 2021, **12**, 12274–12285.
48 J. Liu, I. Craciun, A. Belluati, D. Wu, S. Sieber, T. Einfalt, D. Witzigmann, M. Chami, J. Huwyler and C. G. Palivan, *Nanoscale*, 2020, **12**, 9786–9799.
49 H. Lee, J. Park, N. Kim, W. Youn, G. Yun, S. Y. Han, D. T. Nguyen and I. S. Choi, *Adv. Mater.*, 2022, **34**, 2201247.
50 G. M. Gadd, *Curr. Biol.*, 2021, **31**, R1557–R1563.

